Automot. Engine Technol. (2017) 2:63–77
https://doi.org/10.1007/s41104-017-0019-3

ORIGINAL PAPER

Impact of cyclic lean–rich aging under $DeSO_x$ condition on the lean-gas light-off and hydrogen formation ability of a lean NO_x trap (LNT)

Michael Maurer[1] · Thomas Fortner[1] · Peter Holler[1] · Stefan Zarl[1] · Helmut Eichlseder[2]

Received: 12 December 2016 / Accepted: 15 June 2017 / Published online: 7 July 2017

Abstract In this paper, the aging impact of desulphation ($DeSO_x$) procedures on lean NO_x traps (LNT) was investigated. With accelerated aging procedures on an engine test bench and on a synthetic-gas test bench, LNTs were stressed with lean rich cycling under realistic desulphation conditions. Exhaust gas chassis dynamometer tests showed the impact on emissions of the lean rich treatment. High carbon monoxide (CO) slips were detected in NEDC tests during NO_x regeneration ($DeNO_x$). With light-off tests, the pattern of damage was further investigated. A pronounced deactivation in CO-rich gas conversion was found to be the main reason for the carbon monoxide emissions in the chassis dynamometer tests. A correlation between $DeSO_x$ duration (cumulated duration of rich pulses) and the inhibited CO conversion was observed. Determinations of oxygen storage capacities of aged catalysts indicated that the lean–rich cycling mainly damaged the ceria oxide of the LNT. Variations of the rich gas components indicated that hydrogen in the feed gas as well as in situ generated hydrogen out of feed gas components (steam reforming, water gas shift) is accountable for the degradation in carbon monoxide conversion in rich purges. Investigations for lower desulphation temperatures showed that the effect is negligible for temperature <350 °C. Therefore, catalyst deactivation throughout NO_x regeneration events with much lower temperatures than at $DeSO_x$ was not observed. As reference to other aging treatments used in the literature, samples aged hydrothermally at 750 °C, a phosphorus poisoned and hydrothermally aged LNT as well as a LNT sample from a vehicle endurance run were compared to the $DeSO_x$ aged catalysts. All LNTs had the same conventional LNT coating.

Keywords $DeSO_x$ · Lean–rich cycling · Hydrothermal aging · LNT deactivation · Ceria oxide · WGS · Temperature · Rich gas

Abbreviations

Al_2O_3	Aluminum oxide
BaO	Barium oxide
C_3H_6	Propene
C_xH_y	Hydrocarbon consisting of x carbon- and y hydrogen-atoms
CeO	Ceria oxide
CO	Carbon monoxide
CO_2	Carbon dioxide
$DeNO_x$	Regeneration mode to desorb and reduce stored nitrates from the LNT
$DeSO_x$	Desulphation operation mode to remove sulphur from lean NO_x traps
ECU	Engine control unit
ER	Endurance run
EFTA	European Free Trade Association
EU6	Stage 6 of the European exhaust emissions regulation
EU15	Member states of the European Union since the eastern enlargement 2004
FTIR	Fourier Transform Infrared spectrometer
GHSV	Gas hourly space velocity
H_2	Hydrogen
H_2O	Water/water steam
HC	Hydrocarbons

✉ Michael Maurer
michael.maurer@bmw.com

[1] BMW Group Werk Steyr, Entwicklung Dieselmotor, Steyr, Austria

[2] TU Graz, Institut für Verbrennungskraftmaschinen und Thermodynamik, Graz, Austria

HCOOH	Formic acid
HT	Hydrothermal
LNT	Lean NO_x Trap
MFC	Mass flow controller
N_2	Molecular nitrogen
NDIR	Non dispersive infrared detector
NEDC	New European Driving Cycle
$(NH_4)H_2PO_4$	Ammonium dihydrogen phosphate
NO	Nitrogen monoxide
NO_2	Nitrogen dioxide
NO_x	Collection of all nitrogen oxides (NO, NO_2,…)
PGM	Platin-group-metal
PMA	Paramagnetic detector
OEM	Original equipment manufacturer
O_2	Oxygen
OSC	Oxygen storage capacity
Pd	Palladium
Pt	Platinum
Redox	Reduction oxidation reaction
RDE	Real driving emissions
Rh	Rhodium
SCR	Selective catalytic reduction
THC	Hydrocarbons
T	Temperature
T50	Temperature at 50% conversion in light-off tests
WGS	lean–rich-aging
(g)	Gaseous species
(s)	Surface species

1 Introduction

The share of diesel engines in new passenger cars for the western European market (EU15 + EFTA) was about 53.1% in 2014 corresponding to a report of the European Automobile Manufacturers Association (ACEA). Compared to 1990, where only 13.8% of new passenger cars had diesel engines, the increasing popularity of diesel-driven cars is obvious [1].

Beside the high demand of customers, the diesel engine is essential in the automobile manufacturer's portfolio because of its advantages in thermodynamic efficiency and, therefore, lower CO_2-emissions compared to conventional gasoline engines. Diesel engines are essential to lower the overall fleet CO_2-emissions. A drawback of the diesel engines' lean combustion process is, that conventional three way catalysts cannot be used to reduce engine out NO_x [2–4]. To comply with the current European emissions legislation (EU6) and with further real driving emissions legislation (RDE), complex NO_x exhaust aftertreatment systems are necessary. While the particulate matter problem was solved with the introduction of diesel particulate filters (DPF), current NO_x limits are still a challenge. To achieve the NO_x goals, BMW uses both Lean-NO_x-Traps (LNT) and selective catalytic reduction systems (SCR-systems) [5–7].

The operating principle of Lean NO_x Traps can be separated roughly into a cyclic storage phase of NO_x under lean conditions, where NO_x are adsorbed and bound in form of nitrates, and a reduction phase, where stored NO_x are released and subsequently reduced to N_2 [8, 9]. Depending on the washcoat formulation of the LNT, the maximum in NO_x storage and as a consequence the interval between NO_x-regeneration events varies strongly. When a defined NO_x-storage is reached a regeneration event is necessary [8, 9]. The NO_x regeneration—the so-called $DeNO_x$ event—takes place by a change in engine operating mode. A special combustion setting, the rich mode, leads to a rich exhaust gas with a lambda value <1 [4, 5].

LNTs typically contain NO_x-storage components, like alkali or alkaline earth metals, and precious metals on aluminum oxide [8, 10]. Because of its chemical properties, NO_x traps also operate as sulphur traps. The sulphur is bound as sulphates on the storage components similar to NO_x. Sulphur can originate from fuel or lubricant oil [8, 9]. As both nitrate and sulphate formation takes place on the storage components, increasing sulphur poisoning decreases the maximum in NO_x storage significantly as shown in [11–13]. The sulphating mechanism is reversible [14, 15]. To recover the NO_x-trapping performance of LNTs after sulphur poisoning, another rich engine operation mode, similar to the NO_x regeneration event, is necessary. As sulphates are much more stable than nitrates, higher regeneration temperatures are necessary compared to a $DeNO_x$ event. For efficient desulphation events ($DeSO_x$) different OEMs use periodically triggered particulate filter regeneration events, where LNT temperatures of about 580–630 °C are common. The $DeSO_x$ takes place during the DPF regeneration because no further catalyst heat up is necessary. Depending on the strategy of the particular OEM an substoichiometric exhaust gas (lambda <1) is set up for a defined cumulated time per $DeSO_x$ event with varying pulse duration and number of pulses to release the bound sulphur from the LNT [5, 16, 17].

Beside the so-called sulphur poisoning, the maximum catalyst temperature is an important criterion for Lean NO_x Trap aging. Especially during $DeSO_x$ events it is important to not exceed maximum LNT temperatures [5, 16]. Thermal aging of LNTs primarily takes place at temperatures of 800 °C and above, like shown by Rohr et al. [18]. Despite keeping in the recommended $DeSO_x$ temperature range of LNT suppliers of approximately 700 °C, performance loss of LNTs can be observed over their lifetime. To grow the

knowledge of aging effects and deactivation mechanisms during desulphation events, the impact of excessive $DeSO_x$ throughout cyclic lean–rich pulsing at relevant temperatures has been investigated on an engine test bench and on a synthetic gas test bench. To reveal the impact on the emission performance, chassis dynamometer tests were performed.

2 Experimental methods

2.1 Catalyst samples

Investigations were done on a conventional LNT technology. The LNT washcoat was built up with PGM components platin (Pt), palladium (Pd) and rhodium (Rh), NO_x storage compounds barium oxide (BaO) and ceria oxide (CeO) and remainder aluminum oxide (Al_2O_3). The washcoat was supported on a cordierite monolith with a cell density of 400 cells per square inch.

2.2 Engine test bench aging and chassis dynamometer tests

To investigate the impact of excessive desulphation on a Lean NO_x Trap in automotive usage, a conventional LNT–DPF combination system as used by BMW has been aged on a 3.0-l common-rail diesel engine. The engine was operated cyclically for 40 s in lean heating mode to set a temperature of approximately 620 °C following 14 s in rich mode. During rich mode, the LNT temperature increased because of exothermic reactions. The maximum LNT temperature did not exceed 710 °C to avoid a higher thermal degradation than during endurance runs (Fig. 4). This procedure was repeated for 1500 cycles to reach a cumulated rich time of 21,000 s. This amount is a bit higher than for typical endurance runs but was better suited to detect and understand the aging effects.

The synthetically $DeSO_x$-aged LNT was afterwards installed in a test vehicle with a 3.0-l diesel engine. The LNT performance was determined on an exhaust chassis dynamometer in the New European Driving Cycle (NEDC).

2.3 Synthetic-gas test bench experiments

Furthermore, to determine the aging effects and mechanisms, fresh LNT cores with a diameter of 25.4 and 76.2 mm length from the same production process as the engine test bench $DeSO_x$-aged full part sample were investigated on a synthetic-gas test bench (SG test bench). Figure 1 shows a schematic overview of the experimental setup on the synthetic gas test bench.

Mass flow controllers were used to mix the synthetic gases from gas cylinders. The carrier gas was nitrogen to adjust the defined volume flow. Water and decane were applied in fluid phase, vaporized by evaporator units and added to an additional nitrogen flow that was again added to the before mixed gaseous species. The mass flow controllers and evaporator bank were installed in a redundant circuit. Therefore, two different gas mixtures were available at the same time. Via a switching valve, and it was possible to switch very fast between the two gas mixes to simulate lean–rich cycling as it occurs, when a $DeNO_x$ or $DeSO_x$ event is triggered. The reactor consisted of a quartz-tube flow reactor in a furnace to get an isothermal temperature distribution across the entire LNT sample. To set up the gas temperature a N-type thermocouple was installed 10 mm upstream of the LNT inlet surface (green line in Fig. 1). LNT sample temperature was measured inside a channel with thermocouples placed 3 mm from the inlet as well as from the outlet surface. The thermocouple positions are shown in Fig. 2 in detail. Gas for analysis was taken downstream of the catalyst sample. Hydrocarbon species (C_xH_y) and water content were analyzed with a FTIR spectrometer, total hydrocarbons with a flame ionization detector (FID), carbon monoxide (CO) and carbon dioxide (CO_2) with a nondispersive infrared detector (NDIR), because of its better accuracy, and oxygen with a paramagnetic detector (PMA). Nitrogen oxides (NO_x) were analyzed with a chemiluminescence detector (CLD). For hydrogen determination through electron impact ionization a mass spectrometer was used.

Synthetic-gas test bench aging was analogous to the engine test bench aging. The availability of redundant MFC banks allowed a realistic reproduction of the lean–rich cycling. A gas temperature of 620 °C, for the lean gas as well as the rich gas mix, was set up to get a lean gas and LNT temperature comparable to the engine test bench aging. Lean and rich gas concentrations for the synthetic gas aging were similar to the engine and are listed in Table 1 below.

To determine the impact of desulphation $DeSO_x$ pulse length, the number of $DeSO_x$ pulses and cumulated $DeSO_x$ rich time have been varied. The $DeSO_x$ aged samples were compared to other aging procedures, to classify the aging effects resulting out of excessive desulphation. Two samples were hydrothermally aged for 20, respectively, 110 h at 750 °C on the synthetic gas bench. Another LNT was poisoned with phosphorus and further hydrothermally aged for 20 h at 750 °C, similar to the thermally aged sample. Phosphorus was deposited on the LNT via wet impregnation method with an aqueous solution of ammonium dihydrogen phosphate ($(NH_4)H_2PO_4$), like that used in [19]. To get a reference to the performance after realistic in-car-usage, a LNT from a BMW endurance run with representative full useful life

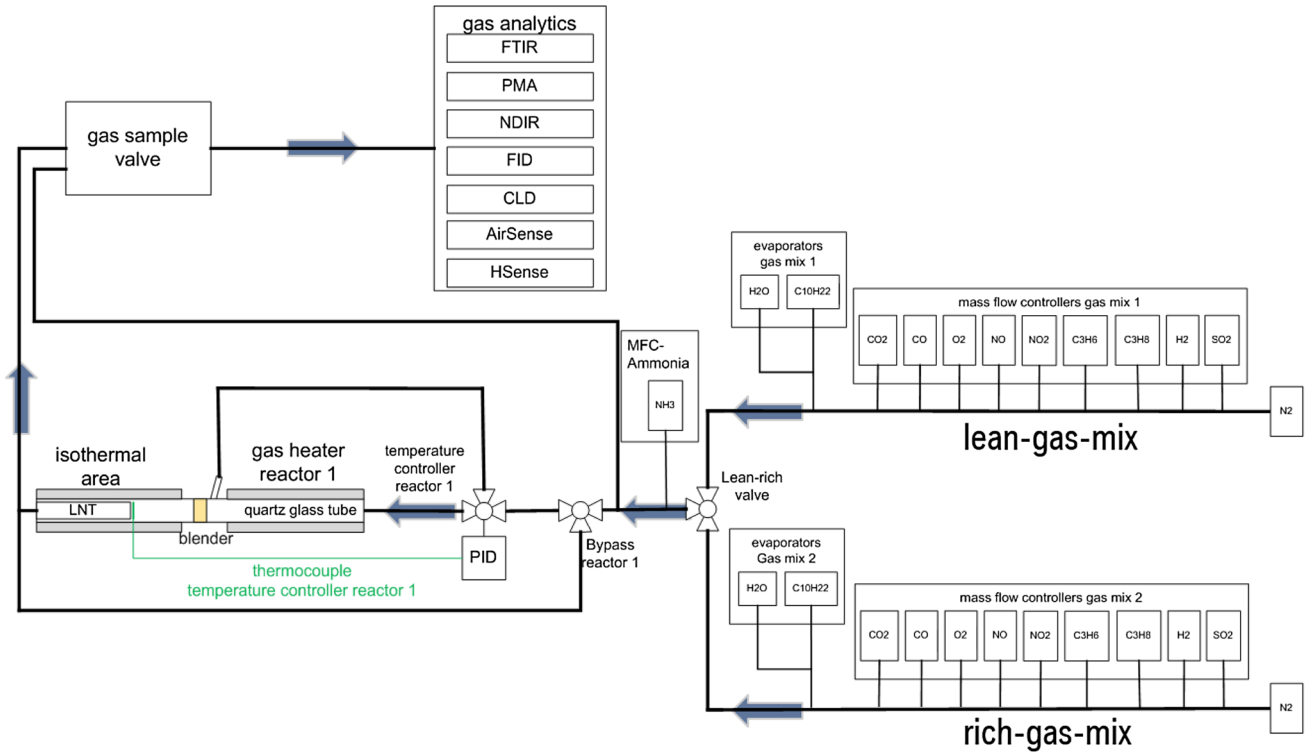

Fig. 1 Schematic of the experimental setup on the synthetic gas test bench

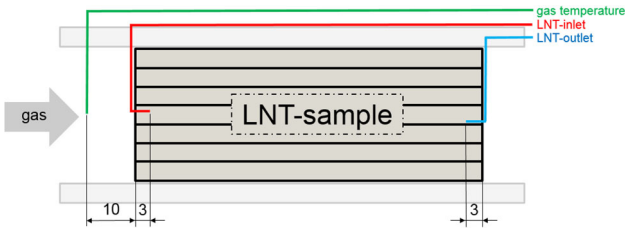

Fig. 2 LNT preparation for synthetic-gas-test-bench experiments. Thermocouples were placed upstream and within the channels of the catalyst sample

Table 1 Lean and rich gas composition for synthetic gas bench $DeSO_x$-aging

Rich gas	Lean gas
12.9% CO_2	11.7% CO_2
10% H_2O	10% H_2O
0.47% O_2	4.3% O_2
200 ppm NO	200 ppm NO
2.7% CO	0.42% CO
1900 ppm C_3H_6	110 ppm C_3H_6
9000 ppm H_2	

performance was uncanned and LNT samples were taken from the full monolith. This sample will be denoted with "ER".

The test array with various $DeSO_x$ aging levels regarding number of pulses and pulse length as well as competitive other aging procedures is shown in Table 2 below. To show the influence of the $DeSO_x$ start temperature (the LNT temperature at the beginning of a rich purge), aging with 14 s pulse length was performed at two further temperatures. The possibility of a lower $DeSO_x$ temperature and the impact of $DeNO_x$ events were verified. Furthermore, rich gas species have been varied in three further agings with 14 s rich pulse length.

$DeSO_x$ aged samples were tested in a defined sequence. In a first step, the samples were aged to reach a defined cumulative rich time. Following this, the sample was tested in a lean gas light-off test, two water gas shift light-off tests with different CO concentrations, $DeNO_x$ efficiency tests (not discussed in this paper) and a determination of the oxygen storage capacity of the catalyst sample. All tests were conducted with a gas hourly space velocity (GHSV) of 40,000 h^{-1}. Before each of the tests the catalyst sample was pretreated with seven lean–rich cycles (120/24 s) at a LNT temperature of 400 °C to get a defined slightly deactivated LNT state. When all tests for one aging iteration were completed, the sample was aged again to reach the next aging state. Figure 3 shows the test sequence. Test conditions for all tests are listed in Table 3.

The hydrothermally aged samples were tested in the same sequence, with hydrothermal treatment at 750 °C

Table 2 aging state of all LNT samples shown in this paper ($DeSO_x$-aged as well as other aging procedures)

Sample ID.	Rich pulse duration Number of rich pulses	7 s	14 s	21 s	Additional information
1	167			3500 s	Gas/LNT temperature: 620 °C
1	500			10,500 s	Gas/LNT temperature: 620 °C
2	750		10,500 s		Gas/LNT temperature: 620 °C
3	750		10,500 s		Gas/LNT temperature: 500 °C
4	750		10,500 s		Gas/LNT temperature: 350 °C
5	750		10,500 s		H_2 as only reductant in the gas feed @620 °C
6	750		10,500 s		CO and H_2 as only reductant in the gas feed @620 °C
7	750		10,500 s		C_3H_6 as only reductant in the gas feed @620 °C
8/1	1000	7000 s		21,000 s	Gas/LNT temperature: 620 °C
8/2	1500	10,500 s	21,000 s		Gas/LNT temperature: 620 °C
3	1500		21,000 s		Gas/LNT temperature: 500 °C
4	1500		21,000 s		Gas/LNT temperature: 350 °C
5	1500		21,000 s		H_2 as only reductant in the gas feed @620 °C after 800 × 14 s CO and H_2
6	1500		21,000 s		CO as only reductant in the gas feed @620 °C after 800 × 14 s CO and H_2
7	1500		21,000 s		C_3H_6 as only reductant in the gas feed @620 °C
8	3000	21,000 s			Gas/LNT temperature: 620 °C
9	20 h@750 °C HT				Hydrothermal aging with 10% H_2O and 10% O_2 at 750 °C LNT temperature for 20 h
10	110 h@750 °C HT				Hydrothermal aging with 10% H_2O and 10% O_2 at 750 °C LNT temperature for 20 h
11	0.2 g/l phosphorus + 20 h@750 °C HT				
ER	Endurance run (ER)				Cum. $DeSO_x$ approx. 7500 s

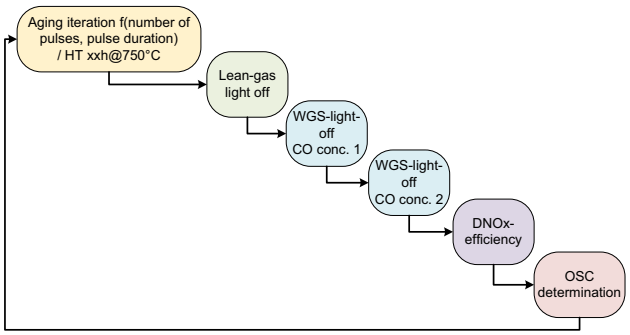

Fig. 3 Test sequence for experiments on the synthetic-gas test bench

instead of $DeSO_x$ aging. The endurance run sample was tested without the aging step.

3 Results

The following section shows the results of engine test bench aging procedure, emission results of tests on the exhaust chassis dynamometer and the results of the synthetic-gas test bench experiments.

3.1 $DeSO_x$ aging procedure on engine test bench

Figure 4 illustrates the LNT in brick temperatures during catalyst aging on the engine test bench. The thermocouple positions are different to the SG test bench setup. The first thermocouple was applied after one-third of the total LNT length, and the second one after two-thirds of the brick length. Throughout aging, the LNT-temperature slowly increased to a maximum bed temperature of 715 °C. The reached maximum temperature is within the recommended operating temperature for this technology. In the literature significant deactivation effects by high-temperature operation were observed at treatments of 5 h at temperatures of 800 °C and above [18]. Thus, a LNT deactivation caused by high temperatures was avoided.

3.2 Emission results of exhaust chassis dynamometer tests

The aged catalyst performance was evaluated in a test vehicle in a NEDC. The test was repeated to avoid inaccuracies of the gas analytics. Figure 5 shows scaled

Table 3 Test conditions for validation of LNT performance after aging on the synthetic gas test bench

Test	Pre-treatment	Temperature	Gas mix
Lean-gas light-off	7 × 24 s rich 120 s lean—400 °C	Temperature programmed 120 → 500 °C 5 °C/min	5.5% CO_2, 6.3% H_2O, 12% O_2, 200 ppm NO, 1500 ppm CO, 116 ppm C_3H_6, 52 ppm C_3H_8, 0% H_2 GHSV: 40,000 h^{-1}
WGS light-off CO conc. 1	7 × 24 s rich 120 s lean—400 °C	Temperature programmed 120 → 500 °C 5 °C/min	0% CO_2, 11.8% H_2O, 0% O_2, 0% NO, 2.15% CO, 0% C_3H_6, 0% H_2 GHSV: 40,000 h^{-1}
WGS light-off CO conc. 2	7 × 24 s rich 120 s lean—400 °C	Temperature programmed 120 → 500 °C 5 °C/min	0% CO_2, 5.6% H_2O, 0% O_2, 0% NO, 5100 ppm CO, 0% C_3H_6, 0% H_2 GHSV: 40,000 h^{-1}
OSC determination	7 × 24 s rich 120 s lean—400 °C	200 °C steady state, 300 °C steady state	120 s O_2 → 60 s N_2 →15 s CO→ 60 s N_2 4.1% O_2, 0% CO in O_2-Phase 0% O_2, 5000 ppm CO in CO-Phase GHSV: 40,000 h^{-1}

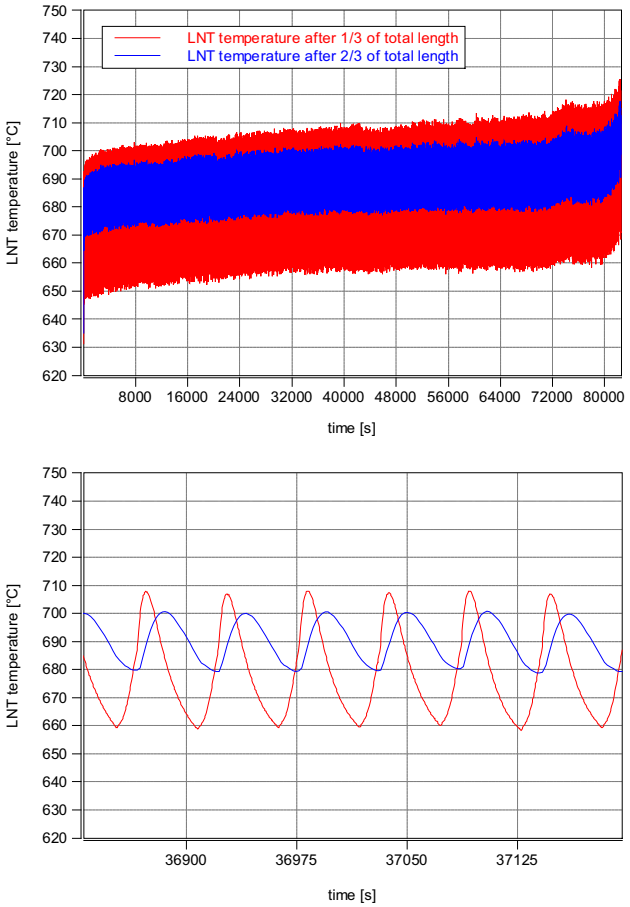

Fig. 4 *Upper part* measured LNT temperatures during $DeSO_x$ aging on a 6-cylinder 3.0-l diesel engine. *Lower part* detailed temperature trends of six $DeSO_x$ pulses

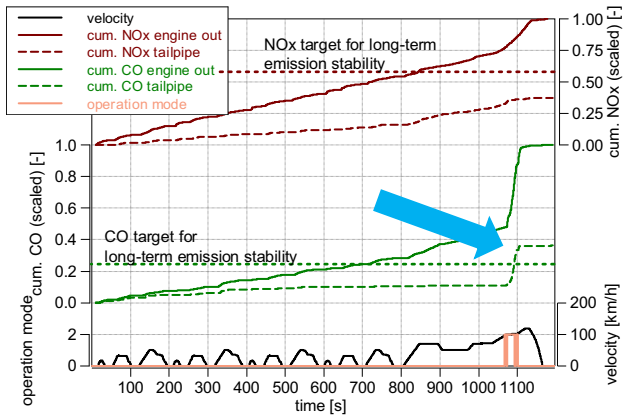

Fig. 5 Scaled cumulated emission trends in NEDC with excessive $DeSO_x$ aged LNT with 1500 pulses with 14 s rich pulse duration (factor 2–3 of a realistic in car aging $DeSO_x$ treatment)

cumulated emissions during a NEDC with the $DeSO_x$ aged LNT. As one can see, the weighted NO_x results in the NEDC are uncritical but CO values are significantly higher than the set targets for long-term emission stability. A detailed consideration of cumulated CO trends in the NEDCs shows that two effects caused the carbon monoxide emissions. First, the CO light off is postponed, so CO is poorly oxidized in the beginning of the test. The second and much more relevant reason for the high CO values was found during the LNT regeneration phase.

Figure 6 shows the $DeNO_x$ event in detail. The upper part of the figure shows the lambda trends during the NO_x regeneration event. The red signal is the lambda value upstream of the LNT, the blue one the downstream lambda signal. A complete NO_x regeneration leads to a sharp decrease in downstream lambda as one can see in the third rich pulse in Fig. 6 (arrow 2). This phenomenon is used to detect a complete $DeNO_x$ event. The behavior of the downstream lambda signal is very untypical (arrow 1). After at least 10 s, a sharp decrease in downstream lambda

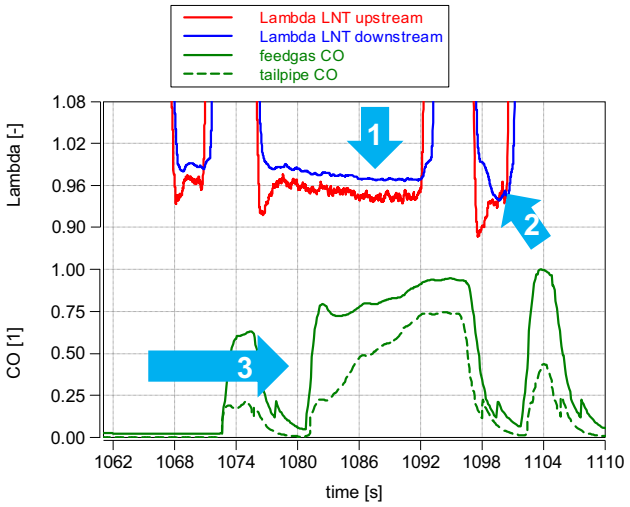

Fig. 6 Scaled CO concentrations of feedgas (*green full line*) and tailpipe (*green dashed line*) emissions during the NO_x regeneration event of NEDC (Fig. 5) and LNT upstream (*red*) and downstream (*blue*) lambda of the $DeSO_x$ aged LNT after 1500 pulses of 14 s

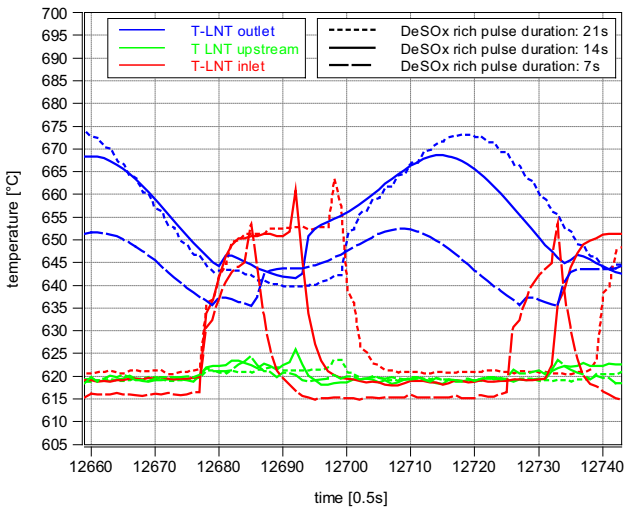

Fig. 7 Comparison of LNT inlet and outlet temperatures with 7, 14 and 21 s $DeSO_x$ pulses during $DeSO_x$ aging cycles on the synthetic gas test bench

caused by slipping rich gas, like CO and mainly hydrogen, would have been expected. As the downstream lambda signal strongly correlates with the hydrogen content in the exhaust gas during a $DeNO_x$ event, increasing hydrogen concentrations would have led to a sharp decrease in the lambda value of the oxygen sensor downstream of the catalyst. Obviously, the LNT was not able to form hydrogen out of the rich gas CO via water gas shift mechanism (explained in detail in Sect. 3.5), leading, as a result, to the high CO slip during the $DeNO_x$ event. CO started to slip very early and nearly reached the feedgas emissions at the end of the second $DeNO_x$ purge as marked with arrow 3.

3.3 Transfer of the aging procedure to the synthetic-gas test bench

To study the deactivation mechanisms the engine test bench procedure was transferred to the synthetic-gas test bench. Figure 7 shows gas and LNT temperatures during one of the $DeSO_x$ aging procedures on the gas test bench. The green line corresponds to the gas temperature upstream of the LNT, the red one to the LNT inlet and the blue one to the LNT outlet temperatures (see Fig. 2) during the aging iterations with a $DeSO_x$ pulse length of 7, 14 and 21 s. For the tests with 7 and 21 s pulses, the gas temperature was set to the same level as during the aging tests with 14 s pulse length, because the $DeSO_x$ start temperature does not depend on the pulse duration when a $DeSO_x$ event is triggered in the car. Exothermic reactions led to different LNT inlet and outlet temperatures at the end of the rich gas purges. Figure 7 shows a comparison of maximum temperature peaks depending on $DeSO_x$ pulse duration. A maximum LNT temperature of 675 °C was not exceeded. A decreasing pulse length led to a lower LNT inlet and outlet temperature. The peak temperature difference between 7 and 21 s $DeSO_x$ pulses was 23 °C.

3.4 Lean gas light off

In Sect. 3.2, a postponed lean gas light off and a strongly inhibited water gas shift reaction during the $DeNO_x$ event are shown for the engine test bench aged sample. To evaluate the influence of $DeSO_x$ pulses on the oxidation behavior, light-off experiments were conducted with a realistic lean gas composition—for details, see Table 3—at a gas hourly space velocity of 40,000 h^{-1}. After lean/rich pretreatment, the LNT was cooled down to 120 °C under pure N_2, then the lean gas was added and the LNT was heated up to 550 °C with 5 °C per minute. Figure 8 shows the light-off temperature for different stages of $DeSO_x$ aging compared to other aging treatments. The shown light-off temperatures are LNT inlet temperatures, where 50% of the dosed gas species (CO or C_3H_6) were oxidized.

Within the group of $DeSO_x$ aged samples, there was no significant difference in CO light-off performance noticeable. Neither the pulse number, nor the pulse length, nor the cumulated rich time had an effect on the light-off temperature. Even after 7000 s $DeSO_x$, all samples showed a comparable performance. Only the sample with 3500 s rich time had a better CO oxidation performance, but worse than the 20-h hydrothermally treated LNTs. The lowest CO light-off temperature was observed with the 20-h hydrothermally aged sample. Although the duration of high-temperature exposure was comparable to the $DeSO_x$ aged samples with 21,000 s cumulated rich time, the 20-h

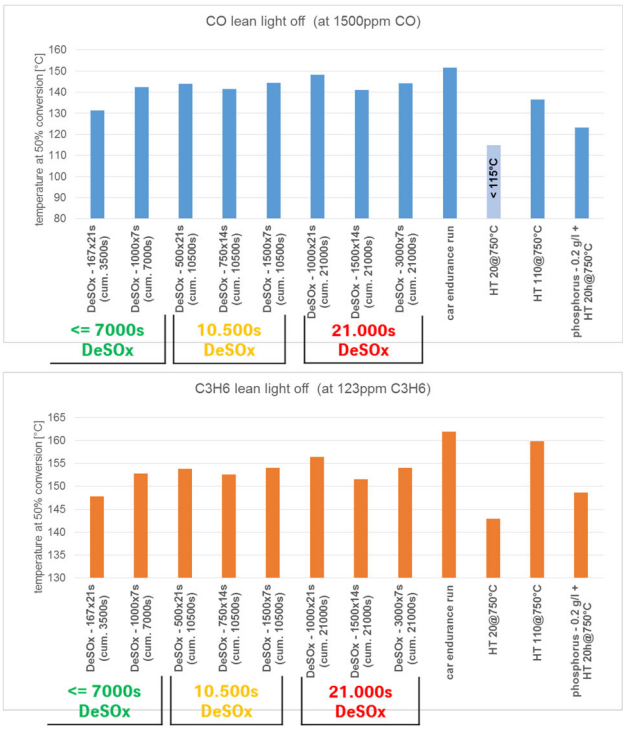

Fig. 8 Light-off temperatures for carbon monoxide and propene in lean gas light-off tests for $DeSO_x$ aged, hydrothermally aged, phosphorus poisoned and hydrothermally aged and realistic aged LNT samples. (*Light blue bars* show light-off temperatures lower than 120 °C)

at 750 °C HT aged LNT had a significant earlier light off. Extended hydrothermal aging with 110 h at 750 °C led to a slightly better CO oxidation than after more than 7000 s $DeSO_x$-rich treatment. The effect of phosphorus poisoning and HT aging was similar to the only HT aged LNT. The small amount of 0.2 g/l phosphorus had only a minor impact on the light-off result. Compared to the realistic aged LNT sample after the endurance run, the $DeSO_x$ aged LNTs showed a similar to slightly better light-off performance. Despite a much lower $DeSO_x$ exposure of approximately 7500 s cumulated rich time, the endurance run sample showed a marginal higher CO light-off temperatures. This behavior can be explained by longer thermal treatment because of DPF soot burning operation, where the LNT reaches approx. 700 °C, and further residual sulfur and phosphorus poisoning, which had been identified by ICP analyses.

The results of propene light-off tests were similar to the CO oxidation results. There is no significant effect of $DeSO_x$ pulse duration, pulse number and cumulated rich time noticeable. The endurance run LNT had the highest light-off temperatures, whereas the 20-h hydrothermally aged sample had the best oxidation characteristics. Only the 110-h hydrothermally aged sample had a performance comparable to the ER sample.

3.5 Hydrogen formation

The main reason for the high carbon monoxide emissions in the exhaust chassis dynamometer tests in Sect. 3.2 was attributed to a poor rich gas conversion during the NO_x regeneration event. As described below, an inhibition of the hydrogen (H_2) formation mechanism was supposed, as no CO was converted and no decrease in downstream lambda was observed. On the one hand, H_2 is a very effective reducing agent, especially at very low $DeNO_x$ temperatures [20–23]; on the other hand, it plays an important role in the detection of a complete NO_x regeneration because of the hydrogen sensitivity of the oxygen [30] sensor downstream of the LNT. Catalytic hydrogen formation over a LNT with a comparable formulation was frequently mentioned in the literature [22, 24–29] and takes place according to the water gas shift (WGS) mechanism (1):

$$CO + H_2O \rightleftarrows CO_2 + H_2. \quad (1)$$

The WGS-mechanism is catalyzed by platin and ceria oxide. With palladium and rhodium as PGM components, good WGS activity was observed too [27]. As Pt is the main PGM component on the investigated LNT washcoat, primarily platin will influence the WGS activity and in the following equations, only Pt is applied. There are two theories discussed in literature how H_2 formation takes place on a LNT. In [27–29] a two-stage redox mechanism is supposed. First, CO adsorbs on platin out of the gas phase (2) and is further oxidized to CO_2 by oxygen from ceria oxide (CeO_2) (3). Over reduced ceria (Ce^{+3}) an O atom is separated from a water molecule and hydrogen gets formed (4).

$$CO(g) + Pt(s) \rightarrow CO - Pt(s) \quad (2)$$

$$CO - Pt(s) + 2CeO_2(s) \rightarrow CO_2(g) + Pt(s) + Ce_2O_3(s) \quad (3)$$

$$Ce_2O_3(s) + H_2O(g) \rightarrow H_2(g) + 2CeO_2(s). \quad (4)$$

A second approach originates from a dissociation of H_2O to OH and H and subsequent formation of HCOOH surface formates with CO that was adsorbed on Pt. With H_2O present in the gas phase, surface formates decompose and H_2 and CO_2 are formed [28, 29]. Jain et al. [29] found that H_2 is formed via both described mechanisms. They came to the conclusion that smaller ceria particles led to lower activation energies regarding H_2 formation. They also proposed that the Pt–CO interaction as well as imperfections in the ceria oxide crystallite (in this case O vacancies) improves water gas shift activity [29]. A determination whether path 1 or path 2 accounts for the investigated LNT formulation cannot be done. It is very likely that both the state of Pt and also the ceria crystallite are responsible for the WGS activity.

To evaluate the effects of $DeSO_x$, hydrothermal aging and chemical poisoning, a WGS light-off test similar to the lean gas light off was carried out. The LNT was pretreated at 400 °C with seven lean–rich cycles, cooled down to 120 °C in nitrogen and then heated up to 500 °C at a rate of 5 °C/min. To investigate only the WGS activity solely CO and H_2O in a balance of N_2 were supplied at a GHSV of 40,000 h^{-1}. The test was done with two different CO to H_2O ratios of 0.51–5.6 and 2.15–11.8%, where the second one is more realistic to a $DeNO_x$ purge in a car.

As shown in Eq. (1) the stoichiometric coefficients of CO_2 and H_2 are the same. It can be assumed that the formation of one CO_2 molecule coincides with one H_2 molecule. Because of the lower drift of the NDIR compared to the HSense during long tests, the CO_2 signals during the WGS light off were compared. From Eq. (1), hydrogen formation during the test is concluded. Figure 9 shows one of the WGS light-off tests in detail. The upper part of the figure shows the gas and LNT temperatures. The curves below show CO, CO_2 and H_2. It can be clearly seen that with increasing temperature, more CO was converted and higher CO_2 concentrations were detected. The increase in CO_2 comes with the same stoichiometric increase in hydrogen as proposed.

Figure 10 shows the CO_2 formation over the LNT inlet temperature of all $DeSO_x$ aged samples. The samples are separated into groups of their cumulated $DeSO_x$ rich time. Red lines show the tests with 21,000 s, blue lines 10,500 s and green line 7000 s or less $DeSO_x$ rich time. Figure 10 contains the test results with the high CO to H_2O ratio. Results of the second CO/H_2O ratio are not shown but had similar results with lower light-off temperatures for all samples.

One can see that WGS activity strongly depends on the cumulated rich time of the $DeSO_x$ aging treatment. The effect of pulse length and total number of $DeSO_x$ rich pulses is negligible compared to the cumulated rich time as will be seen in detail later. To classify the impact of desulphation stress, the $DeSO_x$ aged LNTs were compared to hydrothermal treatment, a combination of phosphorus poisoning and hydrothermal treatment and the endurance run aged LNT in Fig. 11. An evaluation of the ECU data of the endurance run resulted in a cumulated $DeSO_x$ rich time of 7500 s. The result of the endurance run regarding hydrogen formation is in the range of the results of 7000 s $DeSO_x$ aging. The 20-h hydrothermally aged LNT showed a better performance than all other samples. After excessive hydrothermal aging of 110 h at 750 °C, the results were comparable to those after 7000 s $DeSO_x$ or the endurance run. 110 h at temperatures of 750 °C and above are not realistic for a LNT in real driving operation. Therefore, the effect of thermal aging is minor for the inhibited CO conversion like that shown in the $DeNO_x$ event in the NEDCs in Sect. 3.2. In addition, phosphorus poisoning with realistic phosphorus amounts and additional 20 h hydrothermal aging did not lead to same aging in

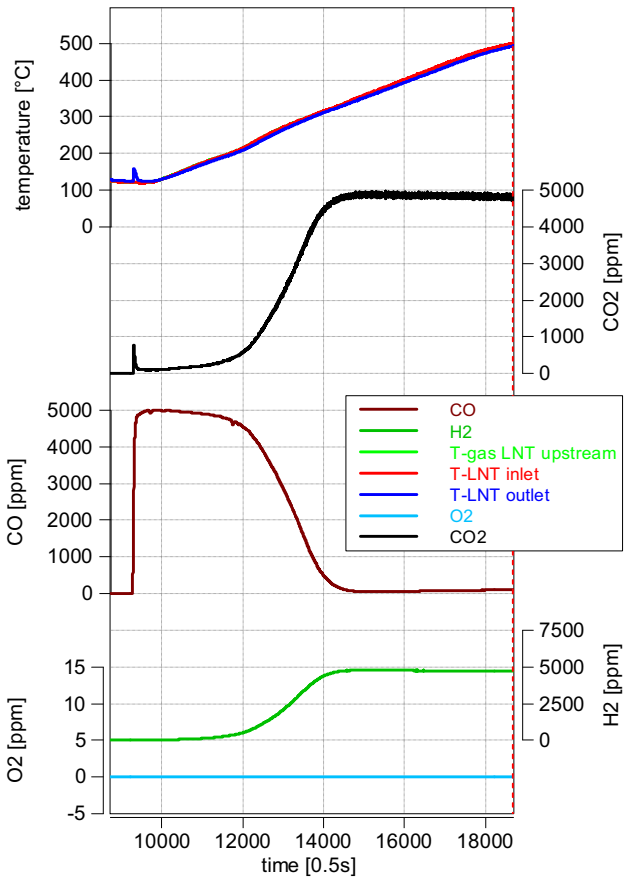

Fig. 9 WGS light-off experiment with start temperature of 120 °C heated up to 500 °C with a rate of 5 °C/min, GHSV 40,000 h^{-1} and 0.51% CO, 5.6% H_2O for the endurance run aged LNT sample

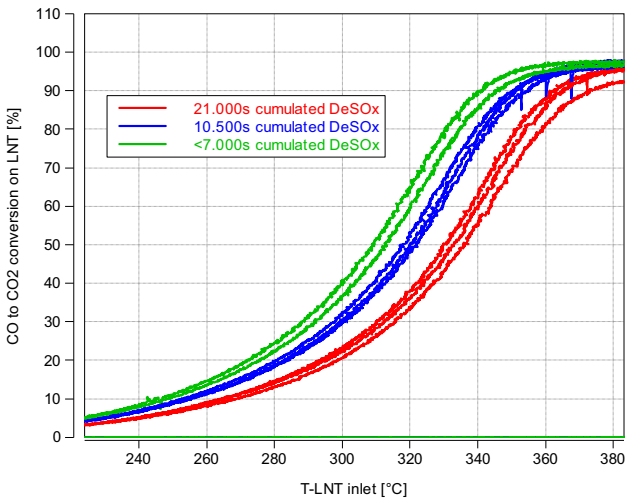

Fig. 10 CO to CO_2 conversion as function of LNT inlet temperature for all $DeSO_x$ aged LNT samples as indicator for hydrogen formation through water gas shift mechanism. Test conditions: GHSV 40,000 h^{-1}; gas feed: 2.15% CO und 11.8% H_2O in a balance of N_2

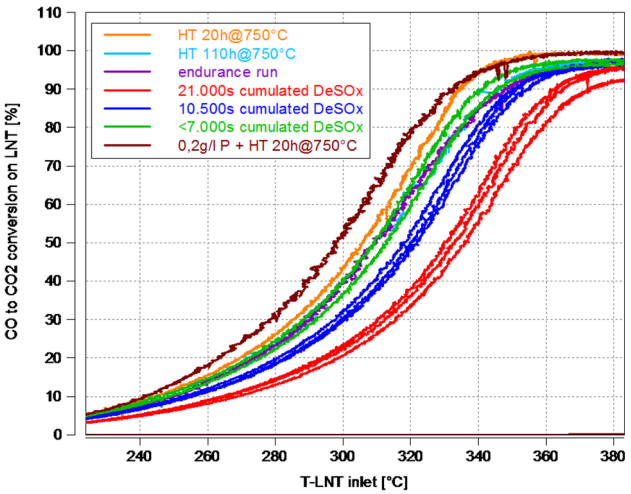

Fig. 11 Comparison of WGS activity of 7 s $DeSO_x$ aged LNT samples with 7000, 10,500 and 21,000 s cumulated rich time to hydrothermal aging, a combination of phosphorus poisoning and hydrothermal and car endurance run aging

WGS activity as after the 10,500 s and 21,000 s of $DeSO_x$-rich treatment.

To show the aging effect in WGS activity during realistic $DeNO_x$ purges like in the New European Driving Cycle, the $DeSO_x$ aged samples with 7 s pulse length were compared to the 20-h@750 °C hydrothermally aged sample in the relevant temperature window (Fig. 12). At a catalyst temperature of 280 °C (vertical black line in Fig. 12) the WGS activity between the four aging iterations strongly differs. The hydrothermal sample converted 27% of the dosed CO to CO_2, what means that 27% of the engine out carbon monoxide is converted to hydrogen with respect to Eq. (1). So, approximately 5800 ppm H_2 was formed, when the feed gas contained 2.15% CO. After

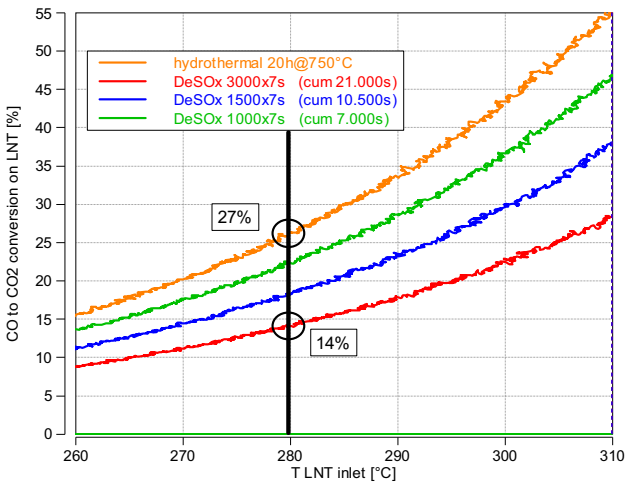

Fig. 12 Impact of $DeSO_x$ aging on CO to CO_2 conversion and further hydrogen formation in the relevant NEDC $DeNO_x$ temperature span and detailed values for 280 °C LNT temperature

21,000 s cumulated $DeSO_x$ rich time only 14% of the feed gas CO was converted, what led to 3000 ppm H_2. The difference of 2800 ppm of hydrogen means that there is less of the most effective reductant available for NO_x reduction. In addition, if a hydrogen sensitivity of 0.01 in lambda for 1500 ppm H_2 is assumed, the deactivation in WGS activity causes a slower lambda decrease and further avoids the detection of a complete $DeNO_x$ event. Therefore, $DeNO_x$ event duration is longer than necessary and the engine out CO slips unconverted and leads to high CO tailpipe emissions.

A detailed comparison of the WGS light-off temperatures shows the addressed correlation between cumulated rich time and WGS activity. It can be clearly seen that increasing rich time causes a drastic shift of hydrogen formation towards higher catalyst temperatures. Compared to the synthetic aging treatments, none of those harmed the LNT in the scale of lean–rich aging at 620 °C. Only the LNT sample from the endurance run showed a comparable result. Different CO to H_2O ratios led to different absolute results but the relative trend stayed unchanged (see Fig. 13).

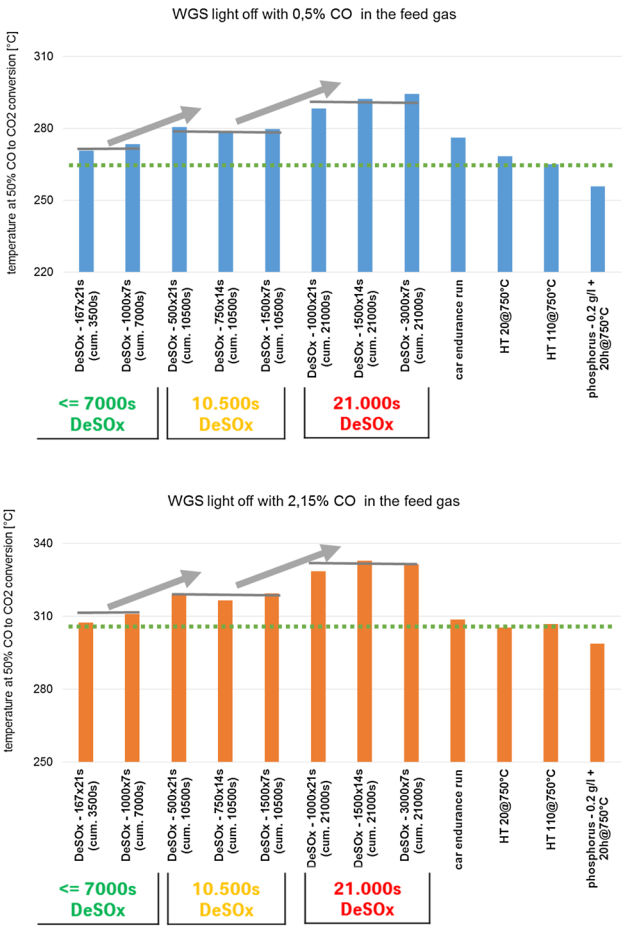

Fig. 13 Detailed results (temperatures at 50% CO and thus H_2 formation) of all WGS light-off tests with 0.5% CO (*blue bars*) and 2.15% CO (*orange bars*)

3.6 Impact of $DeSO_x$ aging on the oxygen storage capacity

Ceria oxide and platinum play an important role for the water gas shift mechanism as mentioned before [27]. A determination of the oxygen storage capacity (OSC) of the LNTs was used as indication whether degradation in ceria oxides occurred. Oxygen storage capacities were determined in a test, where the LNT sample was kept under isothermal conditions at 300 °C. First, the sample was purged with 4% O_2 in a balance of N_2 for 120 s and after 60 s in pure N_2 purged with 5000 ppm CO in N_2 for 15 s. During the phase at which the LNT was purged with oxygen the ceria oxide could oxidize to CeO_2 (Ce^{4+}). The 15-s CO purge led to an oxidation of CO to CO_2 by stored oxygen and a reduction of cerium to Ce_2O_3 (Ce^{3+}). CO was used as reductant as the CO_2 signal quality was better than the H_2O signals from FTIR, when using H_2 as reductant. The higher the OSC of the catalyst the more CO_2 was formed. The forced oxidation and reduction of the cerium was examined in 16 cycles. For a better reproducibility, the last three cycles were evaluated. Figure 14 shows one full cycle of the OSC test procedure (left) and the CO purge in detail on the right side. The influence of $DeSO_x$ aging with 21 s rich purges in contrast to the 20-h hydrothermal treatment is apparent in this graph.

With increasing cumulated $DeSO_x$ rich time the formed CO_2 decreased (Fig. 14 right), what indicated lower oxygen storage capacities. While the LNT aged for 20 h at 750 °C hydrothermally was able to oxidize nearly 50% of the CO, the $DeSO_x$ aged samples had much higher CO slips and, respectively, less CO_2 was formed. The lower oxygen storage capacities with increasing $DeSO_x$ rich time correlates very well with the results from the WGS light-off tests. A detailed view on the maximum CO_2 peaks in the OSC tests showed the same trend as for the WGS light-off charts. The LNT that was aged in the endurance run showed a similar result to that of the WGS light-off tests. Hydrothermally aged samples had much better oxygen storage capacities than $DeSO_x$ aged catalysts. The phosphorus poisoned sample did not cause a degradation of the OSC. A comparison of the CO_2 peak concentration during the CO purge was chosen to be more expressive than the effective amount of CO_2 in mol, as slightly different sample volumes and valve timings could have caused misinterpretation of the data (see Fig. 15).

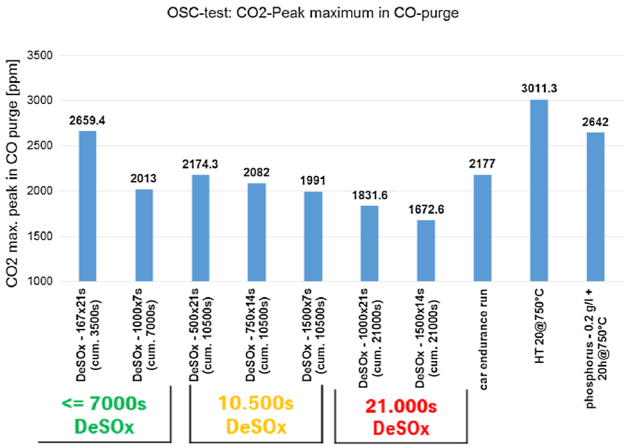

Fig. 15 CO_2 peaks during the CO purge at 300 °C OSC test to determine the oxygen storage capacity of the aged LNTs

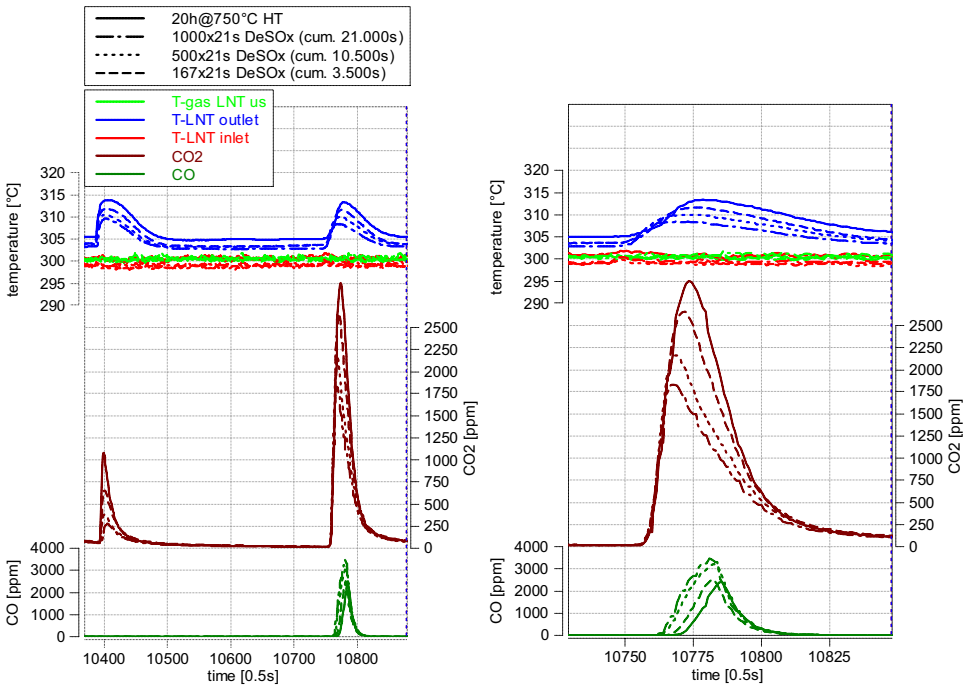

Fig. 14 The *left side* depicts one OSC cycle with an oxidation with 4% O_2 in N_2 and the following reduction with 5000 ppm CO in N_2 of the LNT. The *right part* of the figure shows the CO purge in detail. The difference in CO_2 formation implies a degradation level of the OSC

3.7 Impact of rich gas and aging temperature on WGS activity

To reduce the shown aging effect, three "variables" in the $DeSO_x$ strategy could be adapted. One option is to reduce the cumulated rich time. This will be effective as the deactivation strongly correlates with the cumulated rich time as described in the sections before. Another one would be to lower the $DeSO_x$ start temperature or to change the rich combustion settings, if a specific gas species was reliable for the deactivation effect. Because of this, further tests with different gas mixes as well as lower $DeSO_x$ temperatures have been examined.

3.7.1 Rich gas variation

In a first step, hydrogen and propene were removed from the rich gas mix. Due to the concept of the synthetic-gas test bench, the gas was heated up to approx. 700 °C in the gas heater upstream of the reactor section (see Fig. 1). Even with no hydrogen in the feed, but CO, CO_2 and H_2O an equilibrium reaction in the gas phase led to hydrogen and carbon monoxide equilibrium in the gas feed. So in a first step a gas mix containing CO and lower amounts of hydrogen was used in the lean rich aging. After 830 cycles, the water steam was removed from the feed to prevent hydrogen formation in the gas heater. Therefore, CO was the only rich gas component in the remaining 670 rich cycles. As no water steam was available, hydrogen formation over the LNT was inhibited too for the remaining 670 rich purges. Another test was done with propene as only rich gas component in the rich gas mix. Because of the presence of water in the feed hydrogen was formed over the LNT over the aging procedure. Figure 16 shows the results of the rich gas variations.

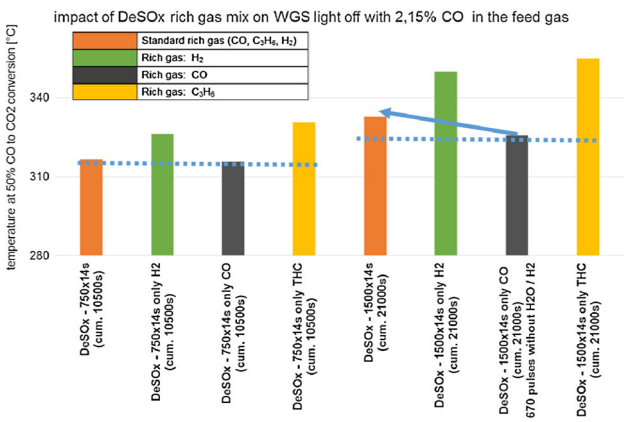

Fig. 16 WGS light-off results with different rich gas mixtures [gray CO with H_2 (first 830 pulses) and CO only (last 670 pulses, respectively, *yellow bars* with propene only and *green bars* with hydrogen as dominating rich gas component]

The WGS light-off tests for the different aging procedures showed two effects. On the one hand, a different mixture of CO and H_2 led to the same degradation as it was seen with the original rich gas (gray and orange bar after 10,500 s rich time). In the absence of hydrogen in the second aging iteration from 10,500 to 21,000 s $DeSO_x$ rich time, the shift of WGS light off was significantly lower compared to the standard rich gas (gray bar in Fig. 16 with 21,000 s rich time from cycle 830 to 1500). Tests with H_2 as major rich gas component (about 2000 ppm CO in the rich gas) resulted in elevated WGS light-off temperatures compared to the original gas mix. The aging treatment with C_3H_6 as single rich gas component led to hydrogen formation over the LNT, without H_2 in the feedgas. This aging treatment had the strongest impact on the WGS light-off temperature, respectively, to the rich gas conversion of the LNT. Summarized, hydrogen seems to have a strong impact on the LNT degradation. H_2 in the feed as well as hydrogen formation over the LNT both harmed the WGS activity of the LNT, whereas catalytic H_2 formation had the strongest effect.

Since in real exhaust gas CO and unburned hydrocarbons always come along with CO_2 and H_2O (the main products of the combustion of hydro carbons), hydrogen formation can not be prevented. A change in the rich combustion will not solve the problem of catalyst deactivation caused by the $DeSO_x$. In addition, hydrogen cannot be removed from real exhaust gas during rich mode.

3.7.2 Reduction of $DeSO_x$ aging temperature

To further investigate whether $DeNO_x$ events also cause the same deactivation as shown with the $DeSO_x$ pulses or a reduction of the $DeSO_x$ temperature avoids the deactivation effect, two more $DeSO_x$ agings at lower catalyst temperatures have been carried out. One test was carried out with a LNT temperature of 350 °C and another one with 500 °C. 500 °C was chosen as very low $DeSO_x$ temperature without considering whether a $DeSO_x$ event will be efficient at these low temperatures. Figures 17 and 18 show detailed WGS light-off results with lowered LNT temperatures.

Figures 17 and 18 show that lean–rich cycling at typical $DeNO_x$ temperatures of 350 °C did not lead to a shift in WGS light off. Although hydrogen formation over the LNT took place at 350 °C during the lean–rich cycling, no degradation effect was noticeable. $DeNO_x$ operation does not harm the LNT. A reduction of the $DeSO_x$ temperature to 500 °C results in a better WGS activity compared to the LNT aged with lean–rich cycles at 620 °C. Compared to the other samples the degradation effect is still significant. 10,500 s cumulated rich time with a $DeSO_x$ start temperature of 500 °C led to the same WGS light off that was shown for the endurance run LNT. A reduction of the

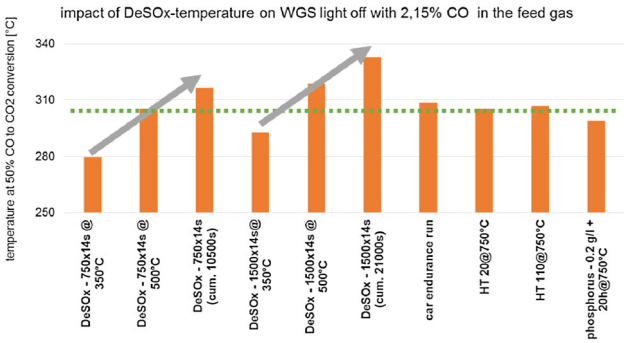

Fig. 17 Results of WGS light-off tests with lower gas and LNT temperatures and 14 s rich pulse length compared to the other aging treatments

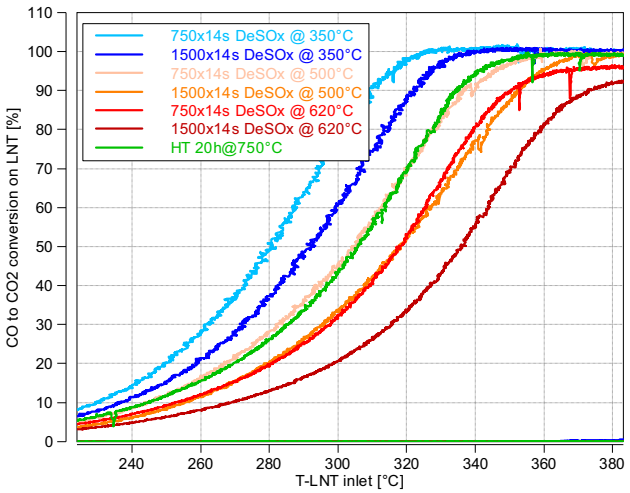

Fig. 18 CO to CO_2 conversion in WGS light-off tests after lean rich cycling at 350, 500 and 620 °C with 14 s pulse length and the CO conversion after 20 h hydrothermal aging at 750 °C as reference

$DeSO_x$ temperature would not have the desired effect of maintaining a sufficient rich gas conversion.

4 Summary and discussion

Accelerated $DeSO_x$ treatment of a LNT on an engine test bench caused high CO emissions in a NEDC on a chassis dynamometer. The reasons were found in a late CO lean light off and mainly in a bad CO conversion during the NO_x regeneration of the LNT. The slope in the lambda signal downstream of the LNT suggested very low hydrogen concentrations. As CO conversion in the rich purge and hydrogen formation occur concurrently relative to the water gas shift mechanism, a deactivation of this specific LNT function was assumed. The deactivation effect of lean–rich cycling at $DeSO_x$ conditions was investigated on a synthetic-gas-test-bench in lean gas light off, WGS light off and oxygen storage capacity tests. The aging procedure of the engine test bench was transferred to the synthetic-gas test bench. To get a reference to the synthetic $DeSO_x$ treatment, the results were compared to a LNT aged in an endurance run under real driving conditions and to other synthetically aged samples, as used in most of the literature studies. The sample aged under realistic conditions in a vehicle endurance run was exposed to approximately 7500 s of $DeSO_x$ rich time. The synthetic aged samples were treated hydrothermally for 20 and 110 h at 750 °C. Another sample was chemically poisoned with 0.2 g/l phosphorus, which represents the same quantity as found on the endurance run sample, and additionally hydrothermally aged for 20 h at 750 °C. Although temperatures in $DeSO_x$ aging procedures on the synthetic gas bench were lower than during the $DeSO_x$ on the engine test bench, a significant impact of the lean–rich treatment was found. While the impact on the propene light off was insignificant, a cumulated rich time of 7000 s led to a shift to higher CO light-off temperatures. Hydrothermal pretreatment with a comparable exposition duration at high temperatures could not reproduce the degradation effect as it was shown with lean–rich cycling. Only at very high expositions like 110 h at 750 °C the deactivation of CO oxidation in a lean gas was comparable. The endurance run sample had the worst CO conversion in lean gas, what was explained by the combination of poisoning, thermal degradation and $DeSO_x$. While the impact on CO light off happened in the first part of the $DeSO_x$ aging, the lean–rich cycling at high temperatures led to a drastic deterioration of CO rich conversion to CO_2 and H_2. Similar to the lean gas light off, there was no clear correlation between pulse number and pulse length. Other than that, the cumulated $DeSO_x$-rich time was a relevant factor regarding hydrogen formation. It is suggested that after more than 21,000 s of cumulated rich time a stronger deactivation would take place. Compared to the hydrothermally aged LNTs, the phosphorus and HT aged sample, none of these samples showed a similar behavior. The endurance run aged LNT fits very well regarding the $DeSO_x$ treatment that has occurred during the endurance run. To prove that lean–rich cycling harms ceria oxide, a test to determine the oxygen storage capacity was done. The results out of OSC tests led to the same trend as the WGS light-off tests. Increasing $DeSO_x$ rich time led to a lower OSC. Samples without lean–rich aging did not show a significant OSC degradation. To show the connection between the OSC of the catalyst and its WGS light-off temperature both values were correlated in Fig. 19.

The correlation between the oxygen storage capacity and the WGS light off can be clearly seen especially for the $DeSO_x$ aged samples. Based on these facts the assumption that the $DeSO_x$ treatment mainly deactivates the ability to

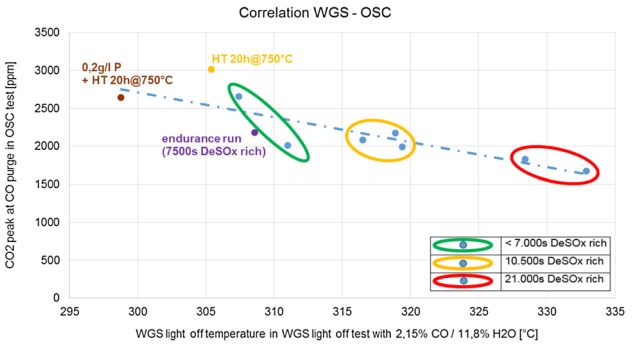

Fig. 19 Correlation between OSC test results and WGS light-off temperatures of $DeSO_x$ aged samples (*green circle* cum. Rich time ≤7000 s, *yellow circle* 10,500 s cum. rich and *red circle* 21,000 s cum. rich) and other aging treatments

convert CO under rich conditions—what is caused by the shift in WGS—was supported.

As $DeSO_x$ is unavoidable when using LNTs, an investigation of the effect of different rich gas mixes was done at 620 °C gas temperature. A test with CO and lower H_2 concentrations led to a similar deactivation effect than with the initial rich gas. By switching off the water dosing unit, hydrogen could be removed from the feed gas. The aging with carbon monoxide as single rich gas component did not lead to a significant further degradation after 670 pulses with 14 s pulse length. As there was no water in the feed, no hydrogen could consequently be formed over the LNT too. A further $DeSO_x$-aging with propene as only rich gas component and no hydrogen in the feed yielded a significant inhibition of the WGS mechanism. Propene, CO_2 and H_2O in the feed gas led to H_2 formation over the LNT. The results from rich gas variations suggested that mainly hydrogen damages the ceria oxide of the lean NO_x trap. Hydrogen formation over the LNT led to an increased performance loss compared to the aging with H_2 in the gas feed. As H_2, CO_2 and H_2O cannot be removed from the engine exhaust gas, the shown deactivation cannot be eliminated by a change in the rich combustion for $DeSO_x$ events.

To investigate the impact of the gas temperature on the LNT deactivation, i.e. whether a reduction in $DeSO_x$ temperature could reduce the aging effect, the lean–rich cycling with 14 s pulses was also done at 350 and 500 °C. While at 350 °C no degradation was observed, 500 °C led to slightly better results than after $DeSO_x$ aging at 620 °C. Although 500 °C is much too low for an efficient desulphation, the result showed that also a reduction of the $DeSO_x$ start temperature could not solve the problem as the catalyst deactivation was much more pronounced than after hydrothermal aging.

Based on these results the absolute necessity of a very efficient $DeSO_x$ strategy was shown. To lower the degradation effect of the LNT, the cumulated $DeSO_x$-rich time per desulphation event was shortened. An effective strategy regarding pulse number and length is under investigation. Further, a Lean NO_x Trap technology that is much more resistant to lean–rich cycling at $DeSO_x$ temperatures was developed by the coating supplier and is currently being tested in endurance runs.

Acknowledgements Open access funding provided by Graz University of Technology.

References

1. European Automobile Manufactorers Association: Share of Diesel in New Passenger Cars, 2015. http://www.acea.be/statistics/article/Share-of-diesel-in-new-passenger-cars. abgerufen am: 13.01.2016
2. Mollenhauer, K. U., Tschöke, H.: (Hrsg.): Handbuch Dieselmotoren. VDI-Buch. Springer, Berlin, Heidelberg (2007)
3. Pischinger, S.: Vieweg Handbuch Kraftfahrzeugtechnik. ATZ/MTZ-Fachbuch. Springer Fachmedien Wiesbaden, Wiesbaden (2016)
4. Hausberger, S.: Skriptum Schadstoffbildung und Emissionsminimierung bei KFZ Teil II. Technische Universität Graz, Graz (2017)
5. Brüne, H.J., Honeder, J., Raschl, P., Schinnerl, M.U., Tangemann, R.: Diesel-Emissionstechniken von BMW für künftige weltweite Abgasnormen. MTZ Motortechnische Zeitschrift **70**(3), S210–S216 (2009)
6. Steinparzer, F., Nefischer, P., Stütz, W., Hiemesch, D. U., Kaufmann, M.: Die neue BMW Sechszylinder Spitzenmotorisierung mit innovativem Aufladekonzept. In: 37. Internationales Wiener Motorensymposium 2016. Wien (2016)
7. Steinparzer, F., Nefischer, P., Hiemesch, D., Kaufmann, M. U., Steinmayr, T.: The New Six-Cylinder Diesel Engines from the BMW In-Line Engine Module. In: 24. Aachener Kolloquium Fahrzeug- und Motorentechnik 2015. Aachen (2015)
8. Epling, W.S., Campbell, L.E., Yezerets, A., Currier, N.W.U., Parks, J.E.: Overview of the fundamental reactions and degradation mechanisms of NO_x storage/reduction catalysts. Catal. Rev. **46**(2), S163–S245 (2004)
9. Takahashi, N., Shinjoh, H., Iijima, T., Suzuki, T., Yamazaki, K., Yokota, K., Suzuki, H., Miyoshi, N., Matsumoto, S.I., Tanizawa, T., Tanaka, T., Tateishi, S.S.U., Kasahara, K.: The new concept 3-way catalyst for automotive lean-burn engine. NO_x storage and reduction catalyst. Catal. Today **27**(1–2), S63–S69 (1996)
10. Matsumoto, S. U., Shinjoh, H.: Dynamic behavior and characterization of automobile catalysts. In: Marin, G. B. (ed.): Advances in chemical engineering. advances in chemical engineering, vol. 33, pp. S1–S279. s.l.: Elsevier textbooks (2008)
11. Engström, P., Amberntsson, A., Skoglundh, M., Fridell, E.U., Smedler, G.: Sulphur dioxide interaction with NO_x storage catalysts. Appl. Catal. B Environ. **22**(4), L241–L248 (1999)
12. Matsumoto, S.: Recent advances in automobile exhaust catalysts. Catal. Today **90**(3–4), 183–190 (2004)

13. Choi, J.S., Partridge, W.P.U., Daw, C.S.: Sulfur impact on NO_x storage, oxygen storage, and ammonia breakthrough during cyclic lean/rich operation of a commercial lean NO_x trap. Appl. Catal. B Environ. **77**(1–2), S145–S156 (2007)
14. Hadl, K., Ratzberger, R., Eichlseder, H., Linares, W., Schüßler, M. U., Bürgler, L.: Grundlegende Betrachtungen zu Ver- und Entschwefelungsmechanismen an NO_x-Speicherkatalysatoren (NSK). In: 9. Internationales Forum Abgas- und Partikel-Emissionen. Ludwigsburg, Deutschland 2016, pp S185–S202
15. Kim, D.H., Yezerets, A., Li, J., Currier, N., Chen, H.-Y., Hess, H., Engelhard, M.H., Muntean, G.G.U., Peden, C.H.: Effect of sulfur loading on the desulfation chemistry of a commercial lean NO_x trap catalyst. Catal. Today **197**(1), S3–S8 (2012)
16. Breitbach, H., Schommers, J., Binz, R., Lindemann, B., Lingens, A.U., Reichel, S.: Brennverfahren und Abgasnachbehandlung im Mercedes-Benz-Bluetec-Konzept. MTZ Motortechnische Zeitschrift **68**(6), S432–S439 (2007)
17. Maroteaux, D., Beaulieu, J.U., D'Oria, S.: Entwicklung der NO_x-Nachbehandlung für Renault-Dieselmotoren. MTZ Motortechnische Zeitschrift **71**(3), S184–S189 (2010)
18. Rohr, F., Grißtede, I., Göbel, U.U., Müller, W.: Dauerhaltbarkeit von NO_x-Nachbehandlungssystemen für Dieselmotoren. MTZ Motortechnische Zeitschrift **69**(3), S212–S219 (2008)
19. Cabello Galisteo, F., López Granados, M., Martín Alonso, D., Mariscal, R.U., Fierro, J.: Loss of NO_x storage capacity of Pt–Ba/Al_2O_3 catalysts due to incorporation of phosphorous. Catal. Commun. **9**(3), S327–S332 (2008)
20. Li, Y., Roth, S., Dettling, J.U., Beutel, T.: Effects of lean/rich timing and nature of reductant on the performance of a NO_x trap catalyst. Top. Catal. **16/17**, S139–S144 (2001)
21. DiGiulio, C.D., Pihl, J.A., Choi, J.-S., Parks, J.E., Lance, M.J., Toops, T.J.U., Amiridis, M.D.: NH_3 formation over a lean NO_x trap (LNT) system. Effects of lean/rich cycle timing and temperature. Appl. Catal. B Environ. **147**, S698–S710 (2014)
22. Abdulhamid, H., Fridell, E.U., Skoglundh, M.: Influence of the type of reducing agent (H_2, CO, C_3H_6 and C_3H_8) on the reduction of stored NO_x in a Pt/BaO/Al_2O_3 model catalyst. Top. Catal. **30/31**, S161–S168 (2004)
23. AL-Harbi, M.U., Epling, W.S.: The effects of regeneration-phase CO and/or H_2 amount on the performance of a NO_x storage/reduction catalyst. Appl. Catal. B Environ. **89**(3–4), S315–S325 (2009)
24. Dasari, P., Muncrief, R.U., Harold, M.P.: Cyclic lean reduction of NO by CO in excess H_2O on Pt–Rh/Ba/Al_2O_3. Elucidating mechanistic features and catalyst performance. Top. Catal. **56**(18–20), 1922–1936 (2013)
25. Limousy, L.: A study of the regeneration of fresh and aged SO_x adsorbers under reducing conditions. Appl. Catal. B **45**(3), 169–179 (2003)
26. Li, J., Theis, J., Chun, W., Goralski, C., Kudla, R., Ura, J., Watkins, W., Chattha, M. U. Hurley, R.: Sulfur poisoning and desulfation of the lean NO_x trap. SAE Technical Paper Series. SAE International 400 Commonwealth Drive, Warrendale, PA, United States (2001)
27. Bunluesin, T., Gorte, R.J.U., Graham, G.W.: Studies of the water-gas-shift reaction on ceria-supported Pt, Pd, and Rh. Implications for oxygen-storage properties. Appl. Catal. B Environ. **15**(1–2), S107–S114 (1998)
28. Jacobs, G.: Water-gas shift. Comparative screening of metal promoters for metal/ceria systems and role of the metal. Appl. Catal. A **258**(2), 203–214 (2004)
29. Jain, R., Poyraz, A.S., Gamliel, D.P., Valla, J., Suib, S.L.U., Maric, R.: Comparative study for low temperature water-gas shift reaction on Pt/ceria catalysts. Role of different ceria supports. Appl. Catal. A Gener. **507**, S1–S13 (2015)
30. Baunach, T., Schänzlin, K.U., Diehl, L.: Sauberes Abgas durch Keramiksensoren. Physik J. **5**, S33–S38 (2006)